Optimal Sampling Strategies for Band-pass Measurement Signals

Leopoldo Angrisani[1], Mauro D'Arco[2], Rosario Schiano Lo Moriello[2], Michele Vadursi[2]

[1] *Dipartimento di Informatica e Sistemistica, Università di Napoli Federico II, 80125 Napoli, Italy*
Phone +390817683170 – Fax +390812396897 – Email: angrisan@unina.it
[2] *Dipartimento di Ingegneria Elettrica, Università di Napoli Federico II, 80125 Napoli, Italy*
Phone +390817683866 – Fax +390812396897 – Email: {darco; rschiano; mvadursi}@unina.it

Abstract- Data Acquisition Systems (DAS) play a fundamental role in a lot of modern measurement solutions. One of the parameters characterizing a DAS is its maximum sampling frequency. As well known from Nyquist theorem, for a correct digitization of analog signals, sampling frequency must be greater than a limit value, related to signal bandwidth. With regard to band-pass signals, which are very common in telecommunications, it is possible to single out some separated ranges of licit sampling frequencies that are significantly lower than such threshold. But, how to choose the sampling frequency conveniently? It seems that there is no instrument currently on the market that selects it properly, given the signal characteristics. The paper proposes a criterion of choice aimed at optimising the DAS resources and two algorithms that perform an automatic selection of the optimal sampling frequency.

I. Introduction

Most modern measurement instruments employed in different application fields consist of an analogue front-end, a data acquisition section (DAS) and a processing section. A key role is played by the DAS, which is mandated to the digitization of input signal, according to a specific sampling frequency. [1,2].
As well known, in order to avoid aliasing, which can seriously affect the accuracy of measurement results, sampling frequency must be adequately chosen. Nyquist theorem, in fact, affirms that a band-limited signal can be alias-free sampled at a frequency f_s greater than twice its highest frequency f_{max}.
With special regard to band-pass signals, which are characterized by a low ratio of bandwidth to carrier frequency and adopted in many telecommunication applications, a much less strict condition applies. For band-pass signals, in fact, the condition to impose is $f_s>B$, B being the signal bilateral bandwidth. It is worth noting, however, that this is only a necessary condition. As a consequence, it is possible to alias-free sample band-pass signals at a frequency f_s much lower than $2f_{max}$, but such frequency has to be chosen very carefully. Some results presented in literature [3-5] show that aliasing can occur even though $f_s>B$; in particular, it occurs if f_s is chosen outside certain ranges.
At the current state of the art, it seems that (i) criteria of choice of f_s among all possible alias-free values have not been put forward, and (ii) digital instruments that automatically select the best f_s, on the basis of specific optimization strategies, given the characteristics of the signal, are not present on the market. Yet, the choice of the sampling frequency is tightly connected to the optimal use of DAS resources, and this is particularly true for modern telecommunication systems, which allocate the spectrum at very high frequencies. The higher the sampling frequency, in fact, the littler the observation time (and the frequency resolution) allowed by the DAS memory buffer.
In the following, a criterion of choice of f_s that meets a very common requirement in electronic measurements and, at the same time, optimizes DAS resources, is proposed. In particular, given the signal bandwidth and the carrier frequency, the idea is to select the minimum value of f_s among those allowed, which implies the allocation of a replica of the spectrum of the analyzed signal at the center frequency chosen by the user. Since the center frequency can be expressed either in Hertz or in normalized terms, two different algorithms have been implemented, which accept the carrier frequency and the signal bandwidth as input, and provide the optimal sampling frequency as output.
The paper is organized as follows. A formalization of the problem, based on straightforward analytical relations, is presented in Section II; analytical details of the two algorithms are given in Section III and the results of some experiments, carried out on actual telecommunication signals with the aim of assessing the reliability and effectiveness of the proposed algorithms, are presented in Section IV.

II. Problem statement

As well known from Nyquist theorem, a band-limited analogue signal $s(t)$, whose highest frequency is f_{max}, can be ideally reconstructed without error from the sequence of its equally spaced samples, if the

sampling frequency satisfies the inequality $f_s > 2f_{max}$. $S_\delta(f)$, the spectrum of the sampled version of $s(t)$, consists of an infinite set of replicas of the spectrum of $s(t)$, centered at integer multiples of f_s, and can be written as

$$S_\delta(f) = f_s \sum_{k \in Z} S(f - kf_s) \quad . \tag{1}$$

Increasing the sampling frequency over $2f_{max}$ results in an increase of the distance between adjacent replicas. The value $2f_{max}$, also called Nyquist frequency, is the threshold over which alias free sampling is guaranteed. On the contrary, when the constraints on the minimum sampling frequency are not satisfied, a fold-over of different replicas can occur (*aliasing*), preventing from a correct reconstruction of the signal.

In the case of a modulated signal, whose spectrum is centered at the carrier frequency f_c, the condition $f_s > 2f_{max}$ can be equivalently written as

$$f_s > 2\left(f_c + \frac{B}{2} \right) \quad , \tag{2}$$

B being the signal's bilateral bandwidth.

Actually, by considering that such signals are characterized by a low ratio of bandwidth to carrier frequency ($B/f_c << 1$), it is possible to adopt sampling frequencies that do not respect condition (2). The spectrum of the original signal is, in fact, practically null in $[0, f_c - B/2]$ thus the superposition of a replica in that sub-band, under certain conditions, does not cause aliasing.

In general, the infinite set of replicas are centered at the frequencies

$$f_{\lambda,\nu} = \lambda f_c + \nu f_s, \quad \nu \in Z, \quad \lambda \in \{-1,1\} \quad . \tag{3}$$

In particular, replicas of the 'positive' spectrum are centered at $f_{1,\nu}$, while replicas of the 'negative' spectrum are centered at $f_{-1,\nu}$. Due to the periodicity of the spectrum of the sampled signal, the analysis can be limited to the interval $[0, f_s]$. It can be shown that only two center frequencies can be found in this interval, f_{λ_1,ν_1} and f_{λ_2,ν_2}; their values are, respectively,

$$f_{\lambda_1,\nu_1} = mod(f_c, f_s) \tag{4.1}$$

and

$$f_{\lambda_2,\nu_2} = f_s - mod(f_c, f_s) \quad , \tag{4.2}$$

where $mod(x,y)$ is the remainder of the ratio x/y. Relations (4.1) and (4.2) show that the two center frequencies are symmetrical with respect to $f_s/2$.

Let us for a moment ignore the case that f_s be a submultiple of f_c, i.e. $f_{\lambda_1,\nu_1} = 0$; then, to avoid superposition of replicas, the following condition has to be respected:

$$\frac{B}{2} < f^* < \frac{f_s - B}{2} \quad , \tag{5}$$

where $f^* = min(f_{\lambda_1,\nu_1}, f_{\lambda_2,\nu_2})$. In other words, due to the symmetry around $f_s/2$, aliasing does not occur if the replica centered in $[0, f_s/2]$ is totally included in that interval. Specifically, with regard to the replica centered at f^*, the two cases respectively shown by Fig.1a and Fig.1b may occur: a) $f^* = f_{\lambda_1,\nu_1}$ and the 'positive' spectrum of the signal $s(t)$ is replicated at f^*; b) $f^* = f_{\lambda_2,\nu_2}$ and the 'negative' spectrum of the signal $s(t)$ is replicated at f^*. Thanks to the hermitianity of $S(f)$, the 'negative' spectrum is the complex conjugate of the 'positive' one and a correct reconstruction of $S(f)$ can be therefore gained by reversing

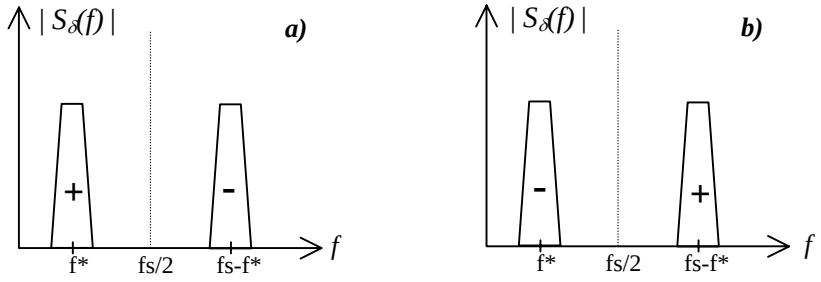

Figure 1. Replicas at the lowest frequency when condition (5) is respected.

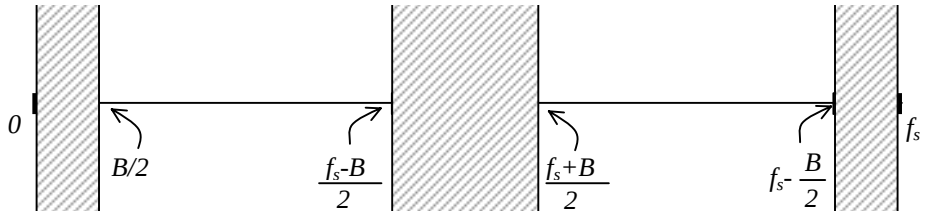

Figure 2. If *mod(f_c,f_s)* is in grey regions, replica superposition occurs.

the order of the acquired samples.
Inequality (5) implies the following condition on mod (f_c, f_s):

$$\mathrm{mod}(f_c, f_s) \in \left(\frac{B}{2}, \frac{f_s - B}{2}\right) \cup \left(\frac{f_s + B}{2}, f_s - \frac{B}{2}\right) \quad . \tag{6}$$

Figure 2 represents the intervals given in (6) as white regions.
Since the bandwidth of a real signal is not strictly limited, a guard band, B_g, between two adjacent replicas is desirable in order to contrast aliasing. Inequality (5) then becomes:

$$\frac{B + B_g}{2} < f^* < \frac{f_s - (B + B_g)}{2} \quad . \tag{7}$$

It can be shown that inequality (5) subtends the necessary condition $f_s > B$.
In the case that f_s be a submultiple of f_c, i.e. $f^* = 0$, the amplitude spectrum shown in Figure 3 is exactly the double of *S(f)* and the phase spectrum is identically null, due to the superposition of the 'positive' and the 'negative' replicas. As a consequence, only measurements on the power spectrum can be performed.
It is worth highlighting that, even though it is possible to sample a band-pass signal at $f_s << 2f_{max}$, with notable advantages in terms of use of DAS resources and costs, the choice of the sampling frequency is not trivial, since a threshold f_t, over which the absence of replica superposition is guaranteed, cannot be singled out.

III. Proposed Strategies

As shown in the previous section, the sampling frequency can be chosen within an infinite set of values and its choice has direct consequences on the spectral allocation of the replicas. On the basis of the relations (3), (4), (5) and (6), the idea is to let the user choose where to center the replica that will be allocated at the lowest frequencies and, consequently, suggest the lowest f_s that satisfies the choice, thus guaranteeing an optimal use of the DAS resources. Specifically, the advantages consist of a reduction of the effects of dynamic non-linearity, as well as of the use of memory resources, given the observation interval.

A. Algorithm I

As it is evident from the relation (3), replicas are not equally spaced on the frequency axis and only one replica is centered in (0,f_s/2); in other words, the normalized frequency f^*/f_s is always < 0.5. The first proposed algorithm allows the choice of the normalized frequency f^*/f_s; specifically, the user can choose f^* in terms of a fraction of f_s. Moreover, the user can input a value for the minimum guard band between adjacent replicas. By imposing

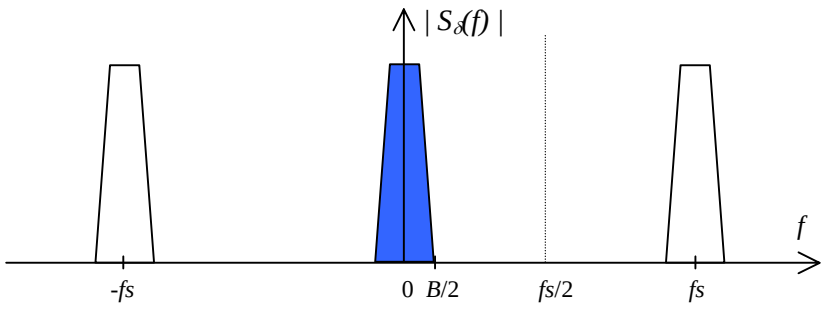

Figure 3. Replicas at lowest frequencies in the case that *mod(fc,fs)*=0.

$$f^* = \frac{f_s}{p}, \quad p > 2 \qquad , \tag{8}$$

inequality (7) reduces to

$$\begin{cases} f_s > \left(B + B_g\right)\dfrac{p}{p-2} & p \le 4 \\ f_s > \left(B + B_g\right)\dfrac{p}{2} & p \ge 4 \end{cases} \qquad . \tag{9}$$

Once the user has entered the desired value for p, algorithm I provides the lowest f_s that verifies (8) and (9), given the bandwidth and the center frequency of the input signal, and the desired guard band between two adjacent replicas, B_g.

Let us impose $f_{\lambda,\nu} = f_s/p$ in (3) and solve the equation with regard to the variable f_s; the equation can be solved when $\lambda = 1$ and $\nu \le 0$, or when $\lambda = -1$ and $\nu \ge 1$. In such cases the unique solution is

$$f_s = \frac{\lambda p}{1 - \nu p} f_c \qquad . \tag{10}$$

The set of possible values for $(1-\nu p)/\lambda p$, arranged in ascending order, is

$$\left\{ \frac{p-1}{p}, \frac{p+1}{p}, \frac{2p-1}{p}, \frac{2p+1}{p}, \ldots, \frac{np-1}{p}, \frac{np+1}{p}, \ldots \right\} \qquad . \tag{11}$$

The algorithm iteratively explores the set of solutions in (11), thus considering each time a lower value for f_s and halts when the current f_s does not respect (9) anymore. The last value of f_s which respects (9) is the lowest sampling frequency that provides the desired positioning of replicas and guarantees the minimum required guard band.

B. Algorithm II

It can be desirable to control the value assumed by f^*, expressed in Hertz, independently from the value of f_s. To this aim, another algorithm is proposed. Given f_c, B, B_g and the desired f^*, it finds (if any) the lowest f_s that gives the desired f^*, while respecting (7).

Let us impose $f_{\lambda,\nu} = f^*$ in (3), and again solve the equation with regard to the variable f_s. If $f^* \in [(B+B_g)/2, f_c]$[1], the equation can be solved when $\lambda = 1$ and $\nu < 0$, or when $\lambda = -1$ and $\nu > 0$. In particular, the possible solutions are

$$f_s = \frac{f^* - \lambda f_c}{\nu} \qquad . \tag{12}$$

Equation (12) yields two infinite sets of possible solutions:

$$\left\{ \frac{f_c + f^*}{\alpha} \right\} \quad \alpha \in N \qquad , \tag{13.1}$$

and

$$\left\{ \frac{f_c - f^*}{\beta} \right\} \quad \beta \in N \qquad . \tag{13.2}$$

Accepted the input parameters, the algorithm checks if the problem admits solutions, i.e. if the left side of the inequality (7) is respected. In case the desired f^* and B_g are incompatible with the given B, an alert message communicates the lowest achievable f^*, given B and B_g and the highest B_g, given B and f^*. If the problem admits solutions, α is initialized at 1 and the algorithm evolves in two steps. At first, α is iteratively increased, as long as the current f_s respects the right side of (7). Then, named $f_s' = \dfrac{f_c + f^*}{\alpha'}$ the lowest valid solution of the first step, β is initialized at the value β_0 that verifies $\dfrac{f_c - f^*}{\beta_0} < f_s' < \dfrac{f_c - f^*}{\beta_0 - 1}$, and is iteratively increased, as long as the current f_s respects the right side of inequality (7).

[1] The case $f^* > f_c$ is not interesting for our purpose and the case $f^* < (B+B_g)/2$ does not respect the left side of (7).

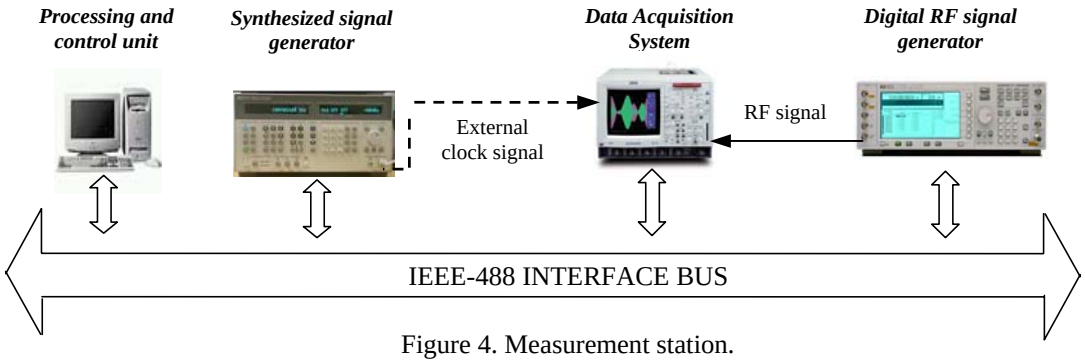

Figure 4. Measurement station.

IV. Experimental Results

A wide experimental activity has been carried out to validate the proposed strategies. At this aim, the measurement station shown in Figure 4 has been set up. It consists of (i) a processing and control unit, namely a personal computer, (ii) a digital RF signal generator (250 kHz-3 GHz output frequency) with arbitrary waveform generation (AWG) capability (14 bit vertical resolution, 1 MSample memory depth, 40 MHz maximum generation frequency), (iii) a data acquisition system (8 bit vertical resolution, 1 GHz bandwidth, 8 GSample/s maximum sample rate, 8 MSample memory depth) and (iv) a synthesized arbitrary waveform generator (0.26-1030 MHz output frequency); they are all interconnected by means of a IEEE-488 standard interface bus.

The validation procedure consists of the following steps: 1) the digital RF signal generator emits a wideband RF signal, characterized by known bandwidth and carrier frequency; 2) given the specified central frequency f^* and guard band B_g, the proposed algorithms provide the optimal sampling frequency f_s; 3) the synthesized signal generator is commanded to output a sinusoidal signal whose frequency value is f_s, in order to drive the DAS sampling clock (external clock); 4) the DAS digitizes the RF signal at a sample rate equal to f_s; 5) the processing and control unit retrieves the acquired samples from the DAS, through the IEEE-488 interface bus; 6) the same unit processes the samples by means of algorithms already presented and validated by the authors [6], in order to estimate the power spectrum of the analysed signal and, finally, 7) assumed the spectrum symmetry, the actual carrier frequency is measured as the threshold frequency that splits up the signal power in halves [7] and then compared to the desired f^*.

QAM (Quadrature Amplitude Modulation) signals adopted for validation are characterized by different bandwidths and carrier frequencies. In particular, imposed values of signal bandwidth and carrier frequency are within, respectively, the range 2 MHz-5 MHz and 200 MHz-500 MHz. Moreover, different values of guard band between replicas have been given in input to the algorithms.

For the sake of clarity, Tables I,II summarize some of the results related, respectively, to algorithm I and algorithm II. Specifically, they are referred to RF signals with B = 5 MHz, and different f_c.

With regard to Table I, the input value for p has been chosen equal to 4, i.e. the desired normalized frequency f^* is 1/4, while different values of guard band have been considered. As for Table II, different values of f^* have been entered in input and a null minimum guard band has been imposed.

It is worth noting that the frequency resolution of the adopted synthesized signal generator, equal to

Table I – Results of the application of algorithm I on RF signals.

	$f^* = 1/4$				
	B_g = 0 MHz	B_g = 5 MHz	B_g = 10 MHz	B_g = 15 MHz	B_g = 20 MHz
	f_c = 300 MHz				
f_s [MHz]	10.084034	20.338984	30.769231	41.379311	52.173914
f^{**}	0.2500011	0.2500006	0.2500000	0.2499999	0.2500001
$\hat{f}^*$	0.2504883	0.2485351	0.2480468	0.2482910	0.2490234
Δ%	0.19%	0.59%	0.78%	0.68%	0.39%
	f_c = 500 MHz				
f_s [MHz]	10.050252	20.202021	30.769231	40.816327	51.282052
f^{**}	0.2500037	0.2500009	0.2499999	0.2499998	0.2500001
$\hat{f}^*$	0.2480468	0.2517089	0.2517089	0.2475586	0.2487793
Δ%	0.78%	0.68%	0.68%	0.98%	0.49%

Table II. – Results of the application of algorithm II on RF signals.

	f^* = 2.5 MHz	f^* = 5 MHz	f^* = 7.5 MHz	f^* = 10 MHz	f^* = 12.5 MHz
	f_c = 300 MHz				
f_s [MHz]	10.083334	15.250000	20.500000	25.833334	31.250000
f^{**} [MHz]	2.500020	5.000000	7.500000	10.000008	12.500000
$\hat{f}^*$ [MHz]	2.518	4.989	7.492	9.984	12.466
Δ%	0.72%	0.22%	0.11%	0.16%	0.27%
	f_c = 500 MHz				
f_s [MHz]	10.050000	15.000000	20.300000	25.500000	30.147059
f^{**} [MHz]	2.500000	5.000000	7.500000	10.000000	12.500003
$\hat{f}^*$ [MHz]	2.495	5.024	7.538	9.986	12.453
Δ%	0.20%	0.48%	0.51%	0.14%	0.38%

1 Hz, has a direct influence on the capability of collocating the spectral replicas at the desired frequencies. Due to such limited resolution, in fact, the sampling frequency, f_s, provided by the algorithms has to be approximated, and the value of the resulting center frequency consequently changes. This is the reason why, together with the desired value of the center frequency given in input, f^*, the tables also report the actual nominal value, f^{**}, resulting from the finite resolution of the adopted synthesized signal generator and obtained by reversely applying the proposed algorithms. Besides f_s, f^* and f^{**}, both tables give the values of $\hat{f}^*$, measured central frequency, and Δ%, relative difference between f^{**} and $\hat{f}^*$, expressed in percentage terms ($\Delta\% = 100\,|\hat{f}^* - f^{**}| / f^{**}$). The results show that Δ% is inside the percentage relative uncertainty, u% (u% within 1-2%), assured by the algorithms for power spectrum estimation [6]. Similar outcomes have been experienced with regard to other RF signals.
Furthermore, the channel power characterising each estimated power spectrum has also been evaluated, with the aim of checking if the spectrum of the replica in [0, f_s/2] suffers from unexpected power level changes. Measurement results, expressed in terms of average value μ and experimental standard deviation σ, have shown that the intervals $[\mu_1 - 3\sigma_1,\ \mu_1 + 3\sigma_1]$ and $[\mu_2 - 3\sigma_2,\ \mu_2 + 3\sigma_2]$, related respectively to the value of channel power provided by the algorithms proposed in [6] and that furnished by a high-performance spectrum analyser, concur, thus highlighting no artful modification of power level.

V. Conclusions

Two algorithms implementing optimal sampling strategies for band-pass measurement signals have been presented and experimentally validated on RF signals. Specifically, the algorithms let the user choose where to collocate the spectrum on the frequency axis and then provide the optimal sampling frequency among those that guarantee the absence of aliasing. The results of a number of experimental tests on RF signals prove that such strategies assure a suitable downconversion of RF signals, since neither the spectrum symmetry nor the power level are unexpectedly modified.

References

[1] J. J. Corcoran, "Analog-to-Digital Converters," Chapter 6 of *Electronic Instrument Handbook C. F. Coombs*, 2nd Edition, McGraw-Hill, 1995.

[2] "Agilent PSA Performance Spectrum Analyzer Series - Measurement Innovation and Benefits", Product Note 1313, Agilent Technologies Literature No.5980-3082EN, 2004.

[3] J. L. Brown, "First-order sampling of bandpass signals-A new approach," *IEEE Transactions on Information Theory*, Vol. 26, No. 5, Sept. 1980, pp.613-615.

[4] R. J. Marks II, *Introduction to Shannon Sampling and Interpolation Theory*, Springer-Verlag, New York 1991.

[5] A. De Paula and R. J. Pieper, "A More Complete Analysis for Subnyquist Band-Pass Sampling," *Proc. of the 24th Southeastern Symp. on System Theory and the 3rd Annual Symp. on Communic., Signal Processing, Expert Systems, and ASIC VLSI Design*, March 1992, pp.20-24.

[6] L. Angrisani, M. D'Apuzzo, M. D'Arco, "A new method for power measurements in digital wireless communication systems," *IEEE Trans. on Instr. and Meas.*, vol.52, No.4, Aug. 2003, pp. 1097-1106.

[7] "Testing and troubleshooting digital RF communications transmitter designs", Application Note 1313, Agilent Technologies Literature No.5968-3578E, 2002.